Cross-Linked Functionalized Poly(3-hexylthiophene) Nanofibers with Tunable Excitonic Coupling

Mina Baghgar,[†] Emily Pentzer,[‡] Adam J. Wise,[§] Joelle A. Labastide,[§] Todd Emrick,[‡] and Michael D. Barnes[†,§,*]

[†]Department of Physics, University of Massachusetts, Amherst, Massachusetts 01003, United States, [‡]Department of Polymer Science and Engineering, University of Massachusetts, Amherst, Massachusetts 01003, United States, and [§]Department of Chemistry, University of Massachusetts, Amherst, Massachusetts 01003, United States

ABSTRACT We show that mechanically and chemically robust functionalized poly(3-hexylthiophene) (P3HT) nanofibers can be made *via* chemical cross-linking. Dramatically different photophysical properties are observed depending on the choice of functionalizing moiety and cross-linking strategy. Starting with two different nanofiber families formed from (a) P3HT-*b*-P3MT or (b) P3HT-*b*-P3ST diblock copolymers, cross-linking to form robust nanowire structures was readily achieved by either a third-party cross-linking agent (hexamethylene diisocyanate, HDI) which links methoxy side chains on the P3MT system, or direct disulfide cross-link for the P3ST system. Although the nanofiber families have similar gross structure (and almost identical pre-cross-linked absorption spectra), they have completely different photophysics as signaled by ensemble and single nanofiber wavelength- and time-resolved photoluminescence as well as transient absorption (visible and near-IR) probes. For the P3ST diblock nanofibers, excitonic coupling appears to be essentially unchanged before and after cross-linking. In contrast, cross-linked P3MT nanofibers show photoluminescence similar in electronic origin, vibronic structure, and lifetime to unaggregated P3HT molecules, *e.g.*, dissolved in an inert polymer matrix, suggesting almost complete extinction of excitonic coupling. We hypothesize that the different photophysical properties can be understood from structural perturbations resulting from the cross-linking: For the P3MT system, the DIC linker induces a high degree of strain on the P3HT aggregate block, thus disrupting both intra- and interchain coupling. For the P3ST system, the spatial extent of the cross-linking is approximately commensurate with the interlamellar spacing, resulting in a minimally perturbed aggregate structure.

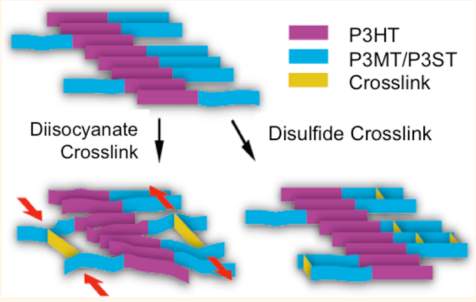

KEYWORDS: P3HT · copolymer · nanofiber · cross-link · exciton coupling · H/J aggregate · photoluminescence

Crystalline 2D nanowires, nanofibers (fibrils) of semiconducting polymers, have attracted a great deal of recent interest for optoelectronic applications such as organic field-effect transistors[1−4] and solar cells.[5−9] Perhaps the most well studied are nanofibers of poly(3-hexylthiophene) (P3HT),[10−12] which are readily formed by self-assembly (crystallization) in a marginal solvent. The balance between inter- and intrachain coupling strength shifts depending upon choice of polymer properties (molecular weight, regioregularity) and choice of solvent.[13−15] The solution-based assembly of these crystalline structures opens new possibilities for controlled interfacing with n-type materials or surfaces, removes the need for post deposition processing of active layers (*i.e.*, annealing), and can give robust nanostructures of controlled electronic properties.[16−19] However, the inherent fragility of these nanowire assemblies is a key limitation, as it makes transfer, mixing, and resuspension in different solvents problematic.

Recently, several groups have explored chemical cross-linking as a means to generate mechanically robust, stable structures for incorporation in solar and optoelectronic devices.[20−22] Polymer cross-linking has been shown to stabilize power conversion efficiencies by minimizing effects of phase-separation in thermal annealing steps of active-layer film preparation.[23] For nanofibers, preserving the pristine aggregate ($\pi-\pi$ stacking) structure and associated intermolecular coupling is seen as essential for efficient long-range charge-transport.[24,25] Recently, Park and Grey have shown how to transfer J-aggregate nanofibers encapsulated

* Address correspondence to mdbarnes@chem.umass.edu.

Received for review July 3, 2013 and accepted September 4, 2013.

Published online September 04, 2013
10.1021/nn403392b

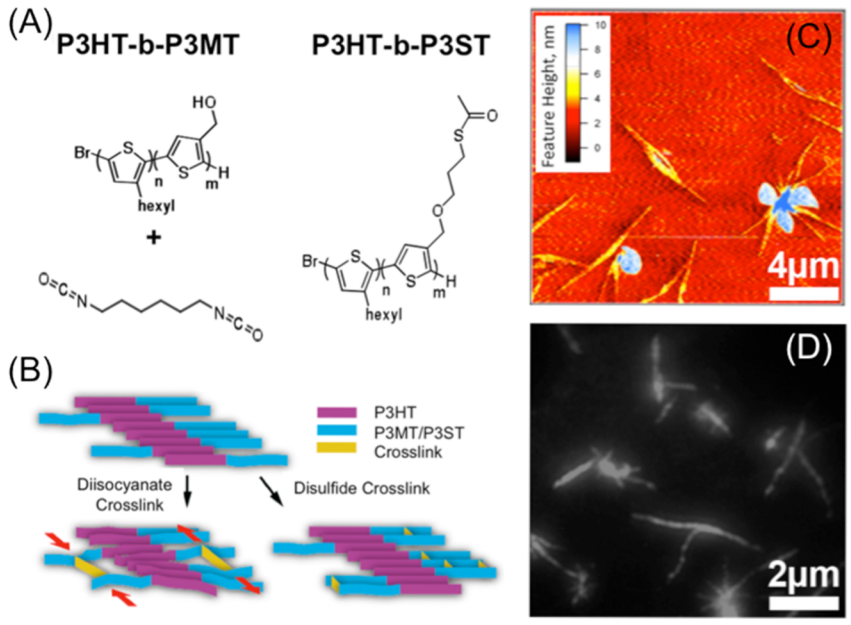

Figure 1. (A) Chemical structures of P3HT-*b*-P3MT/P3ST diblock copolymers and hexylmethylene diisocyanate. (B) Structural schematics of pre- and post-cross-linked nanofibers. Purple bars indicate lamellar assembly of the P3HT blocks, while the blue P3MT (P3ST) blocks participate in the cross-linking (yellow). (C) AFM surface height image of P3MT cross-linked nanofibers showing different morphologies (wires, ribbons, and nanosheet "clover-leaf" structures). (D) Photoluminescence image of dilute P3MT cross-linked nanofibers cast on glass.

in amphiphilic copolymers for transfer/manipulation in different solvent environments.[26] Emrick and coworkers showed that chemical cross-linking of diblock-copolymer nanofibers formed in solution results in mechanically robust, solvent-agile structures that can be cast, resuspended, and/or mixed with a variety of dopants for opto-electronic applications.[20] Of specific interest here is the extent to which cross-linking perturbs the crystalline aggregate, and how different cross-linking strategies might be used to tune electronic properties *via* programmed starting materials and linking agents.

Here, we address the question of how different chemical cross-linking affects exciton coupling in isolated nanofibers. We started with preformed crystalline nanofibers from two different copolymers of similar molecular weight (15 kDa) and molar block ratio (4:1 P3HT/P3XT monomer ratio) in solution: poly-(3-hexylthiophene)-*block*-poly(3-methanolthiophene) (P3HT-*b*-P3MT) and poly(3-hexylthiophene)-*block*-poly-(3-hexylthioacetate thiophene) (P3HT-*b*-P3ST). P3HT-*b*-P3MT nanofibers were cross-linked by addition of hexylmethylene diisocyanate (HDI), while P3HT-*b*-P3ST nanofibers were cross-linked *via* removal of the acetate and oxidation to form disulfide bonds. For simplicity, we identify each diblock copolymer nanofiber family by their polymer functional group: hydroxyl nanofibers (P3MT) and thiol nanofibers (P3ST).

Figure 1 shows monomer structures of the different copolymers and cross-linking agents used in this study, along with a schematic drawing of the corresponding two cross-linked nanofiber families. Low molecular weight polymers were chosen to minimize the possibility of chain folding within the lamellar sheets that occurs when polymer molecular weight exceeds the critical value (typically about 20 kDa in nanofiber structure).[14,27,28] Therefore, P3MT and P3ST functional blocks attached to the end of P3HT chains are unlikely to be present in the fiber core, and only decorate its exterior.[6] Thus, cross-linking the nanofibers composed of lower molecular weight polymer avoids potentially deleterious defects associated with higher molecular weight systems. Photoluminescence images of isolated cross-linked P3MT nanofibers show that their extended structure is maintained through the cross-linking process (Figure 1D). In addition, it is unlikely that the minority block of the copolymer has any intrinsic effect on the electronic structure, as solution phase measurements of absorption and emission of solvated single diblock-copolymer chains show virtually no change as compared to solvated pristine P3HT, although the chemical modifications of the side chains can be seen in IR absorption.

Interestingly, although the suspended-phase absorption spectra of both nanofiber families before and after cross-linking are identical, the nanofiber photoluminescence spectra show a strong dependence on the choice of linker and solvent, where the changes in the 0–0 origin and relative intensities of vibronic sidebands indicate significant variations in exciton coupling. In the cross-linked P3MT nanofibers, time-resolved photoluminescence reports the absence of a fast PL decay component usually associated with crystallinity, in contrast to cross-linked P3ST nanofibers. The observed

differences in photophysical properties between the two cross-liked nanofiber families are mostly owing to the size of the cross-linkage: In the case of P3MT, the cross-linking group that connects polymer chains is longer than the combined hexyl groups of the P3HT structure. Therefore, the linker could react with methoxy groups on the P3MT block on either adjacent or non-adjacent sheets, resulting in a combined "pushing" or "pulling" on the P3HT blocks that disrupt the crystalline packing, thereby weakening both intra- and interchain exciton couplings. In contrast, for the P3ST system, the spatial extent of the cross-linker is commensurate with the interlamellar spacing, resulting in a mild (if detectable) perturbation in the P3HT aggregate structure. Transient absorption measurements of ground-state bleach recovery and polaron absorption (of particular interest in solar cell applications) also reveal the lack of a polaron absorption band in cross-linked P3MT nanofibers that might be due to interrupted exciton coupling across the chain in π-stacks. These combined results demonstrate both physical robustness and electronic tunability in this important class of nanoscale electronic materials.

RESULTS AND DISCUSSION

Figure 2 shows the steady state suspended-phase UV−vis absorption and solid-state photoluminescence spectra of P3MT and P3ST diblock copolymer nanofibers before and after cross-linking. Both diblock copolymer nanofibers have absorption spectra similar to pristine P3HT nanofibers of similar molecular weight (Supporting Information, Figure S2). Prior to cross-linking, the 0−0/0−1 intensity ratios in absorption are characteristic of a weakly coupled H-aggregate ($J_0 \approx +20$ meV).[30] In photoluminescence, the emission spectrum for the P3ST system is essentially unchanged before and after cross-linking, indicating a minimal structural perturbation of the aggregate structure. In contrast, the emission spectra from P3MT nanofibers change dramatically after cross-linking. The polymer chain packing structure appears significantly altered, as evidenced by a change in the 0−0/0−1 intensity ratios from about 1 to 1.4 and a blue shift of ~40 nm in the spectral origin. It should be also noted that the apparent electronic origin at 610 nm for the cross-linked P3MT nanofibers is significantly lower in energy than the corresponding electronic origin of solvated P3HT chains (580 nm), but higher in energy than that in the aggregated film (650 nm). This shift is comparable to that observed for single P3HT chains suspended in a thin film of UHMW polyethylene,[33] despite being in a dense physical aggregate of several hundred nanometers-micrometers in length.

The line shape of the emission spectrum of cross-linked P3MT nanofibers introduces the question of whether interrupted aggregation has changed the dominant chromophore coupling from H to J-type, or

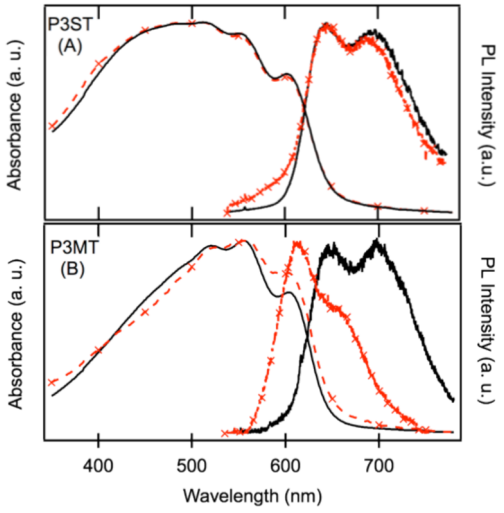

Figure 2. Normalized steady state absorption and emission spectra of (A) P3ST NFs and (B) P3MT NFs before (black) and after (red) cross-linking. Note the significant 40 nm blue shift on the PL spectrum of the cross-linked P3MT nanofibers with respect to 0−0 origins of P3MT nanofibers despite their almost identical absorption spectra.

simply eliminated any H-type aggregate by perturbing interchain communication. In the latter case, the interchain excitonic coupling would be weakened by the change in the spacing between adjacent polymer chains followed by an increase in the torsional disorder which would cause the PL spectral line shape to look like a J-type aggregate with a much smaller stokes shift. On the other hand, cross-linking has a negligible effect on the steady state spectra of diblock copolymer P3ST nanofibers, leading us to conclude that cross-linking by oxidation of thiols to disulfide bonds generates minimal structural perturbation and instead locks in the highly aggregated nanofiber structure without causing major interruption in interchain electronic communication.

In the H/J aggregate model, this observed increase in the 0−0 peaks for the P3MT nanofibers implies that the *intra*chain bandwidth is now larger relative to the interchain bandwidth.[31,32] The observed increase in the PL intensity is also likely a result of a relatively larger reduction in the interchain coupling, consistent with the blueshift in the origin luminescence. If the interchain coupling is reduced, then the spectral separation between the higher-energy absorbing state and the lower-energy emitting state caused by interchain coupling is also reduced, causing a blue shift in the emitting state as the band narrows. This picture is also consistent with the observed reduction in the Stokes shift upon cross-linking. While intrachain disorder is likely increased (in the P3MT system) due to a disruption in π-stacking, these measurements show that the associated reduction in the intrachain bandwidth is *smaller* than the reduction in the interchain bandwidth.

Figure 3 shows a comparison of time-resolved PL from the two families of pre- and post-cross-linked diblock copolymer nanofibers. One of the most striking

features of the time-resolved photoluminescence of the P3MT cross-linked system is the complete absence of the fast PL decay component, suggestive of disruption of crystalline packing in the nanostructure. In this case, the PL kinetics closely resemble that of isolated P3HT chains in chloroform solution or regiorandom P3HT despite physical aggregation into dense bundles of nanofibers. For the cross-linked P3ST nanofibers, a minimal effect on the fast PL decay transient indicates yet again that there is no significant change in intermolecular coupling upon cross-linking. The observed slight decrease in lifetime at very short times might reveal a small increase or a subtle change in electronic coupling.

A fast PL decay component is regarded as one of the characteristic signatures of highly ordered pristine P3HT aggregates and nanofibers, however the mechanism(s) underlying this process remain unclear.[33−37] In previous measurements in our laboratory, we observed that the fast PL decay was highly polarized along the crystallographic *c*-axis (transverse to the nanofiber long axis),

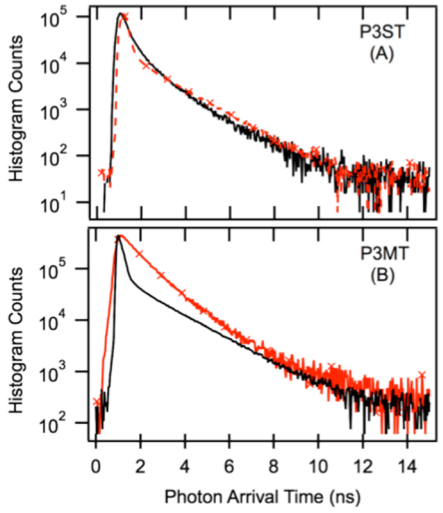

Figure 3. PL Decay traces from 15 kDa P3ST (upper) and P3MT (lower) diblock-copolymer NFs before (black) and after (red) cross-linking. Note the disappearance of the fast decay component for the P3MT system after cross-linking.

suggestive of a correlation with a high degree of intrachain order in these systems.[35] This is supported by measurements on high molecular-weight P3HT nanofibers formed *via* a thermal crystallization in toluene, which show PL spectra characteristic of J-aggregates as a result of their emission and absorption spectra, which display this extremely fast decay mechanism.[36] Thus, we conclude that the disappearance of the fast decay component in the P3MT cross-linked nanofibers is likely a consequence of the interruption of interchain order.[33,34]

To further understand the nature of nanofiber structural perturbation driven by diisocyanate linking, we conducted transient absorption measurements on P3MT nanofibers before and after cross-linking (Figure 4A). Before cross-linking, the transient absorption spectrum consists mainly of a strong ground-state bleach (400−600 nm), along with a broad polaron absorption band centered at 650 nm. This polaron-related absorption band appears to be a generic feature of conjugated polymers and was originally posited to be a SOMO → LUMO transition unique to conjugated polymers that stack into lamellar crystals, with a corresponding HOMO-1 → HOMO transition in the infrared.[38−40] Illuminating work by Noone and Ginger suggests that this feature may be due to electroabsorption rather than true polaron absorption.[7] Interestingly, after cross-linking, this polaron absorption band disappears completely, replaced with a weak bleach band; this new band is most likely stimulated emission, given its energy relative to the overlaid PL spectrum. The complete disappearance of the polaron absorption band after cross-linking may be explained by the fluence-specific transient absorption kinetics (Figure 4B). Cross-linking slows the decay kinetics and reduces the effect of pump fluence. At higher pump fluences, excited states are known to either interact and annihilate or form free charges or polarons.[41] We conclude that the reduction of intermolecular coupling as a result of cross-linking P3MT nanofibers reduces exciton−exciton interaction by confining the exciton to single chains, or perhaps even single chromophores. As a result,

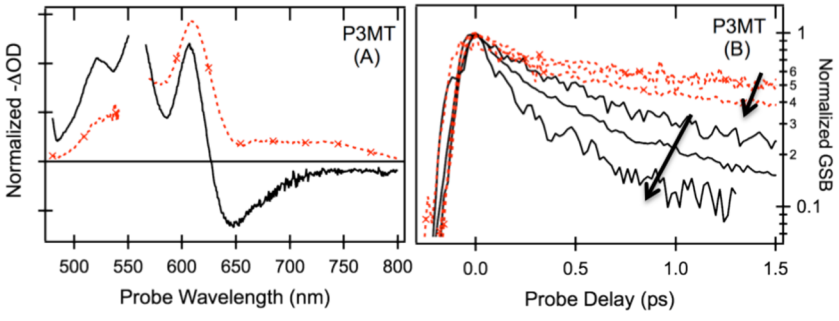

Figure 4. (A) Transient absorption spectra of pre- (black) and post-cross-linked (red) P3MT nanofibers. Horizontal solid line indicates zero TA value. Note the disappearance of the polaron-associated absorption (650 nm) after cross-linking. (B) Ground-state bleach (GSB) kinetic traces of pre- and post-cross-linked P3MT nanofibers as a function of increasing pump fluence (7, 235, and 525 μJ before cross-linking; 15, 65, and 900 μJ after cross-linking. λ_{Probe} = 550 nm). The GSB for pre-cross-linked NFs shows a strong sensitivity to pump fluence (black), while the post-cross-linked NFs are essentially unaffected (red).

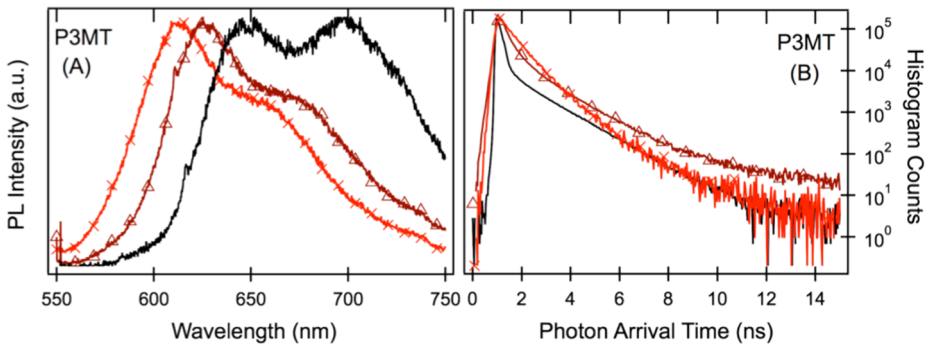

Figure 5. Solvent dependence on (A) room temperature normalized emission spectra, and (B) PL decay dynamics of cross-linked P3MT nanofibers. PL spectra and decay curves from pre-cross-linked NFs are shown in black; post-cross-linked suspended in 1:7 chloroform/dichloromethane (light red crosses), and chloroform (dark red triangles).

even at extremely high pump fluence (nearly 1 mJ/cm^2) there is only weak exciton−exciton annihilation, a process that appears to have a fluence threshold of $\approx 10^{-2}$ mJ/cm^2 in high intermolecular-coupling P3HT aggregates (*i.e.*, un-cross-linked nanofibers).[42,43] Under these experimental conditions, intermolecular interaction is reduced and exciton diffusion is limited, factors that would certainly hinder effective charge separation at the donor/acceptor interface and should be avoided to maximize solar cell efficiency. We do note that the fluences involved in the transient absorption measurements (as well as time-resolved photoluminescence) are many orders of magnitude higher than normal solar illumination, even with intense concentration.

Figure 5A shows the solid-state photoluminescence spectra of P3MT nanofibers before cross-linking (in 1:7 $CHCl_3$/DCM), after cross-linking (in 1:7 $CHCl_3$/DCM), and after cross-linking with solvent exchanged for chloroform (a good solvent for P3HT). Resuspending non-cross-linked diblock copolymer nanofibers in chloroform dissolves the nanofiber completely, returning the emission to a 580 nm electronic origin. In contrast, PL spectra of cross-linked P3MT nanofibers show not only that aggregation remains in chloroform, but also that suspension in a chloroform bath and subsequent recasting into a thin film causes an increase in planarity relative to suspension in chloroform−dichloromethane mixed solvent (1:7 volume ratio) evidenced by a 20 nm red shift of the PL electronic origin. We believe this structural relaxation is caused by relief of strain imposed originally by cross-linking of nonadjacent block copolymer molecules. Suspension in a good solvent (like chloroform) may allow individual chains to move within the constraints of their cross-linking towards a thermodynamically more favorable shape, which results in a longer mean conjugation length and resultant spectral red shift in PL. This effect indicates that the structure within the cross-linked system can still be manipulated by postprocessing, without dissolving the aggregate entirely. This is consistent with the picture of the cross-linked aggregate as a system mechanically constrained only on one edge (the P3MT block side), while the rest of the polymer retains mobility. This view is supported by observation of the absorption spectrum of suspended cross-linked P3MT nanofibers in chloroform, as it shows a strong amorphous component (450 nm) despite few or no free polymer molecules in solution, as the liquid phase of the solvent around the cross-linked fiber bundles remains completely colorless (Supporting Information, Figure S3). Time-resolved PL transients of cross-linked P3MT show that this 'solvent-annealing' process reintroduces some level of interchain aggregation, as the fast component of the decay is restored almost completely (Figure 5B).

Finally, it is useful to try to reconcile the combined spectral and time-resolved data with a structural picture of the two different cross-linked nanofiber families. The photophysical data clearly indicate a strongly perturbed aggregate structure for the cross-linked P3MT nanofibers, and a minimally perturbed structure for the P3ST nanofibers. We believe the fundamental structural differences derive from the nature of cross-linking: The 'third-party' ICN cross-linker accesses primarily methoxy groups on the exterior of the nanofiber. The length of the external ICN linker is such that it favors binding across lamellar sheets, thus functioning as kind of an 'alligator-clip'. For binding between adjacent sheets, the physical size of the linker stresses the sheets apart, while for binding between non-adjacent sheets, there is a pulling effect further distorting the aggregate structure. Grey and co-workers observed similar structural perturbations on single nanofibers by applying high pressure, which exerts a torque on the chain ends thus disrupting the J-aggregation.[36] For the P3ST system, the nature of the cross-linker facilitates almost exclusive linkage between adjacent lamellar sheets, where the length of the cross-linkage is approximately commensurate with the (unperturbed) lamellar spacing.

CONCLUSIONS

We have shown by a variety of photophysical metrics that by controlling the size of the cross-linking

agent relative to alkyl side chain length, exciton coupling in P3HT nanofibers can be controlled, either by including a relatively large linker, which reduces interchain coupling, or alternatively using a linker of comparable length to the lamellar spacing which minimally perturbs the aggregate structure. We are currently exploring the use of intermediate-length linkers to reliably induce more subtle changes in coupling, rather than the gross differences reported above. The ability to lock conjugated polymer structures of interest in photovoltaic devices before or during the mixing of donor and acceptor (or multiple donor, *etc.*) without compromising nanostructure integrity represents a new and potentially useful tool for optimizing solar cell performance. This cross-linking process removes the need for all structures to be kinetically stable at every step during device fabrication, which may include immersion in several solvents, thermal annealing, and bombardment by reactive metal vapor for electrode deposition. We have also shown that the structures formed *via* cross-linking can be 'programmed' with particular levels of strain-induced disorder, and subsequently annealed *via* facile solvent processing. This may be useful for engineering cascades of aggregates without resorting to complicated chemical synthetic procedures, or modification of the surface or particular parts of the device with the introduction of small amount of solvent.

SYNTHESIS AND MATERIALS

P3HT-*b*-P3MT Fibrils. The diblock copolymer P3HT-*b*-P3MT was synthesized as previously reported.[20] The block copolymer used in these experiments had a molar ratio of 4:1 P3HT/P3MT (determined by ^{1}H NMR spectroscopy), M_n = 14 kDa, and PDI = 1.44. The fibrils were prepared as previously reported. In brief, the block copolymer (10 mg) was dissolved in ACS grade chloroform (1 mL) and gently sonicated and heated to 30 °C for 1 h. The solution was then passed through a syringe filter (0.45 μm) into a clean vial, and 7 mL of dichloromethane was added to induce fibrilization. The solution was left in the dark, undisturbed, for 24 h after which 5 mL of the deep purple, opaque solution was added to 800 mL of dichloromethane. Freshly distilled anhydrous triethylamine (1 mL) and hexamethylene diisocyanate (0.1 mL) were then added, and the clear, purple solution was stirred at room temperature in the dark for 12 h. After this time, the deep purple fibrils were floating in the solution, and the solvent was clear. The fibrils were used directly, or isolated by centrifugation at 1000 rpm for 10 min to float the fibrils and removal of the solvent by pipet. The isolated fibrils were then resuspended in the desired solvent.

P3HT-*b*-P3ST Fibrils. P3HT-*b*-P3ST was synthesized as previously reported. The block copolymer used in these experiments had a molar ratio of 4:1 P3HT/P3ST (determined by ^{1}H NMR spectroscopy), M_n = 15.4 kDa, and PDI = 1.28. Fibrils of P3HT-*b*-P3ST were prepared by charging a vial with a stir bar, the block copolymer (5 mg), and anisole (10 mL), then sealing with a Teflon-coated cap and heating to 80 °C in an oil bath until the solution turned bright orange and all polymer was dissolved (approximately 20 min). The heat was then turned off and the oil bath allowed to cool to room temperature after which the vial was removed and placed in a cold room (4 °C) for 8 h. The solution became dark purple and slightly viscous during this time. The fibril solution was diluted with 550 mL of anisole, diethylamine (10 mL, 2.0 M in tetrahydrofuran) was added, and the solution was stirred in the dark for 12 h. After this time, the solution was used as prepared without further processing.

Conflict of Interest: The authors declare no competing financial interest.

Acknowledgment. The transient absorption measurements were carried out at the Center for Functional Nanomaterials, Brookhaven National Laboratory, which is supported by the U.S. Department of Energy, Office of Basic Energy Sciences, under Contract No. DE-AC02-98CH10886. Authors would like to thank Matthew Sfeir for assisting with transient absorption measurements. M.D.B., J.A.L., and M.B. acknowledge support from US Department of Energy under Grant No. DE-FG02-05ER15695 (Program Manager: Larry Rahn). E.P. and A.J.W. were supported by Polymer-Based Materials for Harvesting Solar Energy, an Energy Frontier Research Center funded by the U.S. Department of Energy, Office of Basic Energy Sciences under Award Number DE-SC0001087.

Supporting Information Available: Optical images of cross-linked nanofibers in different solvents, steady state absorption and emission spectra of 13 kDa P3HT polymer and nanofibers. This material is available free of charge *via* the Internet at http://pubs.acs.org.

REFERENCES AND NOTES

1. Chou, C. C.; Wu, H. C.; Lin, C. J.; Ghelichkhani, E.; Chen, W. C. Morphology and Field-Effect Transistor Characteristics of Electrospun Nanofibers Prepared From Crystalline Poly-(3-hexylthiophene) and Polyacrylate Blends. *Macromol. Chem. Phys.* **2013**, *214*, 751–760.
2. Lin, J. C.; Lee, W. Y.; Wu, H. C.; Chou, C. C.; Chiu, Y. C.; Sun, Y. S.; Chen, W. C. Morphology and Field-Effect Transistor Characteristics of Semicrystalline Poly(3-hexylthiophene) and Poly(stearyl acrylate) Blend Nanowires. *J. Mater. Chem.* **2012**, *22*, 14682–14690.
3. Mele, E.; Lezzi, F.; Polini, A.; Altamura, D.; Giannini, C.; Pisignano, D. Enhanced Charge-Carrier Mobility in Polymer Nanofibers Realized by Solvent-Resistant Soft Nanolithography. *J. Mater. Chem.* **2012**, *22*, 18051–18056.
4. Zhou, M.; Aryal, M.; Mielczarek, K.; Zakhidov, A.; Hu, W. Hole Mobility Enhancement by Chain Alignment in Nanoimprinted Poly(3-hexylthiophene) Nanogratings for Organic Electronics. *J. Vac. Sci. Technol., B* **2010**, *28*, C6m63–C66m67.
5. Singh, S.; Vardeny, Z. V. Ultrafast Transient Spectroscopy of Polymer/Fullerene Blends for Organic Photovoltaic Applications. *Materials* **2013**, *6*, 897–910.
6. Cowan, S. R.; Banerji, N.; Leong, W. L.; Heeger, A. J. Charge Formation, Recombination, and Sweep-Out Dynamics in Organic Solar Cells. *Adv. Funct. Mater.* **2012**, *22*, 1116–1128.
7. Noone, K. M.; Subramaniyan, S.; Zhang, Q. F.; Cao, G. Z.; Jenekhe, S. A.; Ginger, D. S. Photoinduced Charge Transfer and Polaron Dynamics in Polymer and Hybrid Photovoltaic Thin Films: Organic *vs* Inorganic Acceptors. *J. Phys. Chem. C* **2011**, *115*, 24403–24410.
8. Briseno, A. L.; Kim, F. S.; Babel, A.; Xia, Y. N.; Jenekhe, S. A. n-Channel Polymer Thin Film Transistors with Long-Term Air-Stability and Durability and Their Use in Complementary Inverters. *J. Mater. Chem.* **2011**, *21*, 16461–16466.
9. Wu, P. T.; Xin, H.; Kim, F. S.; Ren, G. Q.; Jenekhe, S. A. Regioregular Poly(3-pentylthiophene): Synthesis, Self-Assembly of Nanowires, High-Mobility Field-Effect Transistors, and Efficient Photovoltaic Cells. *Macromolecules* **2009**, *42*, 8817–8826.
10. Briseno, A. L.; Mannsfeld, S. C. B.; Shamberger, P. J.; Ohuchi, F. S.; Bao, Z. N.; Jenekhe, S. A.; Xia, Y. N. Self-Assembly, Molecular Packing, and Electron Transport in N-Type Polymer Semiconductor Nanobelts. *Chem. Mater.* **2008**, *20*, 4712–4719.

11. Zhang, Y. J.; Dong, H. L.; Tang, Q. X.; Ferdous, S.; Liu, F.; Mannsfeld, S. C. B.; Hu, W. P.; Briseno, A. L. Organic Single-Crystalline p-n Junction Nanoribbons. *J. Am. Chem. Soc.* **2010**, *132*, 11580–11584.
12. Berson, S.; De Bettignies, R.; Bailly, S.; Guillerez, S. Poly (3-hexylthiophene) Fibers for Photovoltaic Applications. *Adv. Funct. Mater.* **2007**, *17*, 1377–1384.
13. Roehling, J. D.; Arslan, I.; Moule, A. J. Controlling Microstructure in Poly(3-hexylthiophene) Nanofibers. *J. Mater. Chem.* **2012**, *22*, 2498–2506.
14. Brinkmann, M. Structure and Morphology Control in Thin Films of Regioregular Poly(3-hexylthiophene). *J. Polym. Sci., Part B: Polym. Phys.* **2011**, *49*, 1218–1233.
15. Chuangchote, S.; Fujita, M.; Sagawa, T.; Sakaguchi, H.; Yoshikawa, S. Control of Self Organization in Conjugated Polymer Fibers. *ACS Appl. Mater. Interfaces* **2010**, *2*, 2995–2997.
16. Stranks, S. D.; Yong, C. K.; Alexander-Webber, J. A.; Weisspfennig, C.; Johnston, M. B.; Herz, L. M.; Nicholas, R. J. Nanoengineering Coaxial Carbon Nanotube-Dual-Polymer Heterostructures. *ACS Nano* **2012**, *6*, 6058–6066.
17. Pentzer, E. B.; Bokel, F. A.; Hayward, R. C.; Emrick, T. Nanocomposite "Superhighways" by Solution Assembly of Semiconductor Nanostructures with Ligand-Functionalized Conjugated Polymers. *Adv. Mater.* **2012**, *24*, 2254–2258.
18. Bu, L. J.; Pentzer, E.; Bokel, F. A.; Emrick, T.; Hayward, R. C. Growth of Polythiophene/Perylene Tetracarboxydiimide Donor/Acceptor Shish-Kebab Nanostructures by Coupled Crystal Modification. *ACS Nano* **2012**, *6*, 10924–10929.
19. Bokel, F. A.; Sudeep, P. K.; Pentzer, E.; Emrick, T.; Hayward, R. C. Assembly of Poly(3-hexylthiophene)/CdSe Hybrid Nanowires by Cocrystallization. *Macromolecules* **2011**, *44*, 1768–1770.
20. Hammer, B. A. G.; Bokel, F. A.; Hayward, R. C.; Emrick, T. Cross-Linked Conjugated Polymer Fibrils: Robust Nanowires from Functional Polythiophene Diblock Copolymers. *Chem. Mater.* **2011**, *23*, 4250–4256.
21. Wu, F. I.; Dodda, R.; Reddy, D. S.; Shu, C. F. Synthesis and Characterization Of Spiro-Linked Poly(terfluorene): A Blue-Emitting Polymer with Controlled Conjugated Length. *J. Mater. Chem.* **2002**, *12*, 2893–2897.
22. Ma, B. W.; Kim, B. J.; Poulsen, D. A.; Pastine, S. J.; Frechet, J. M. J. Multifunctional Crosslinkable Iridium Complexes as Hole Transporting/Electron Blocking and Emitting Materials for Solution-Processed Multilayer Organic Light-Emitting Diodes. *Adv. Funct. Mater.* **2009**, *19*, 1024–1031.
23. Kim, H. J.; Han, A. R.; Cho, C. H.; Kang, H.; Cho, H. H.; Lee, M. Y.; Frechet, J. M. J.; Oh, J. H.; Kim, B. J. Solvent-Resistant Organic Transistors and Thermally Stable Organic Photovoltaics Based on Cross-Linkable Conjugated Polymers. *Chem. Mater.* **2012**, *24*, 215–221.
24. Kim, F. S.; Jenekhe, S. A. Charge Transport in Poly-(3-Butylthiophene) Nanowires and Their Nanocomposites with an Insulating Polymer. *Macromolecules* **2012**, *45*, 7514–7519.
25. Kim, K.; Lee, J. W.; Lee, S. H.; Lee, Y. B.; Cho, E. H.; Noh, H. S.; Jo, S. G.; Joo, J. Nanoscale Optical and Photoresponsive Electrical Properties of P3HT and PCBM Composite Nanowires. *Org. Electron.* **2011**, *12*, 1695–1700.
26. Gao, J.; Kamps, A.; Park, S. J.; Grey, J. K. Encapsulation of Poly(3-hexylthiophene) J-Aggregate Nanofibers with an Amphiphilic Block Copolymer. *Langmuir* **2012**, *28*, 16401–16407.
27. Zhang, R.; *et al.* Nanostructure Dependence of Field-Effect Mobility in Regioregular Poly(3-hexylthiophene) Thin Film Field Effect Transistors. *J. Am. Chem. Soc.* **2006**, *128*, 3480–3481.
28. Mena-Osteritz, E.; Meyer, A.; Langeveld-Voss, B. M. W.; Janssen, R. A. J.; Meijer, E. W.; Bauerle, P. Two-Dimensional Crystals of Poly(3-alkylthiophene)S: Direct Visualization of Polymer Folds in Submolecular Resolution. *Angew. Chem., Int. Ed.* **2000**, *39*, 2680–2684.
29. Gao, Y. Q.; Grey, J. K. Resonance Chemical Imaging of Polythiophene/Fullerene Photovoltaic Thin Films: Mapping Morphology-Dependent Aggregated and Unaggregated C═C Species. *J. Am. Chem. Soc.* **2009**, *131*, 9654–9662.
30. Spano, F. C. The Spectral Signatures of Frenkel Polarons in H- and J-Aggregates. *Acc. Chem. Res.* **2010**, *43*, 429–439.
31. Tempelaar, R.; Stradomska, A.; Knoester, J.; Spano, F. C. Anatomy of an Exciton: Vibrational Distortion and Exciton Coherence in H- and J-Aggregates. *J. Phys. Chem. B* **2013**, *117*, 457–466.
32. Yamagata, H.; Spano, F. C. Interplay between Intrachain and Interchain Interactions in Semiconducting Polymer Assemblies: The HJ-Aggregate Model. *J. Chem. Phys.* **2012**, *136* (18), 184901–184915.
33. Parkinson, P.; Muller, C.; Stingelin, N.; Johnston, M. B.; Herz, L. M. Role of Ultrafast Torsional Relaxation in the Emission from Polythiophene Aggregates. *J. Phys. Chem. Lett.* **2010**, *1*, 2788–2792.
34. Ferreira, B.; da Silva, P. F.; de Melo, J. S. S.; Pina, J.; Macanita, A. Excited-State Dynamics and Self-Organization of Poly-(3-Hexylthiophene) (P3HT) in Solution and Thin Films. *J. Phys. Chem. B* **2012**, *116*, 2347–2355.
35. Labastide, J. A.; Baghgar, M.; McKenna, A.; Barnes, M. D. Time- and Polarization-Resolved Photoluminescence Decay from Isolated Polythiophene (P3HT) Nanofibers. *J. Phys. Chem. C* **2012**, *116*, 23803–23811.
36. Niles, E. T.; Roehling, J. D.; Yamagata, H.; Wise, A. J.; Spano, F. C.; Moule, A. J.; Grey, J. K. J-Aggregate Behavior in Poly-3-hexylthiophene Nanofibers. *J. Phys. Chem. Lett.* **2012**, *3*, 259–263.
37. Banerji, N.; Cowan, S.; Vauthey, E.; Heeger, A. J. Ultrafast Relaxation of the Poly(3-hexylthiophene) Emission Spectrum. *J. Phys. Chem. C* **2011**, *115*, 9726–9739.
38. Jiang, X. M.; Osterbacka, R.; An, C. P.; Vardeny, Z. V. Photoexcitations in Regio-Regular and Regio-Random Polythiophene Films. *Synth. Met.* **2003**, *137*, 1465–1468.
39. Jiang, X. M.; Osterbacka, R.; Korovyanko, O.; An, C. P.; Horovitz, B.; Janssen, R. A. J.; Vardeny, Z. V. Spectroscopic Studies of Photoexcitations in Regioregular and Regiorandom Polythiophene Films. *Adv. Funct. Mater.* **2002**, *12*, 587–597.
40. Osterbacka, R.; An, C. P.; Jiang, X. M.; Vardeny, Z. V. Two-Dimensional Electronic Excitations in Self-Assembled Conjugated Polymer Nanocrystals. *Science* **2000**, *287* (5454), 839–842.
41. Guo, J. M.; Ohkita, H.; Benten, H.; Ito, S. Near-IR Femtosecond Transient Absorption Spectroscopy of Ultrafast Polaron and Triplet Exciton Formation in Polythiophene Films with Different Regioregularities. *J. Am. Chem. Soc.* **2009**, *131*, 16869–16880.
42. Ohkita, H.; Kosaka, J.; Guo, J.; Benten, H.; Ito, S. Charge Generation Dynamics in Polymer/Polymer Solar Cells Studied by Transient Absorption Spectroscopy. *J. Photonics Energy* **2011**, 1.
43. Guo, J. M.; Ohkita, H.; Yokoya, S.; Benten, H.; Ito, S. Bimodal Polarons and Hole Transport in Poly(3-hexylthiophene): Fullerene Blend Films. *J. Am. Chem. Soc.* **2010**, *132*, 9631–9637.